

On the balance energy and nuclear dynamics in peripheral heavy-ion collisions

Rajiv Chugh and Rajeev K. Puri*

*Department of Physics, Panjab University,
Chandigarh -160 014, India.*

We present here the system size dependence of balance energy for semi-central and peripheral collisions using quantum molecular dynamics model. For this study, the reactions of $Ne^{20}+Ne^{20}$, $Ca^{40}+Ca^{40}$, $Ni^{58}+Ni^{58}$, $Nb^{93}+Nb^{93}$, $Xe^{131}+Xe^{131}$ and $Au^{197}+Au^{197}$ are simulated at different incident energies and impact parameters. A hard equation of state along with nucleon-nucleon cross-sections between 40 - 55 mb explains the data nicely. Interestingly, balance energy follows a power law $\propto A^\tau$ for the mass dependence at all colliding geometries. The power factor τ is close to $-\frac{1}{3}$ in central collisions whereas it is $-\frac{2}{3}$ for peripheral collisions suggesting stronger system size dependence at peripheral geometries. This also suggests that in the absence of momentum dependent interactions, Coulomb's interaction plays an exceedingly significant role. These results are further analyzed for nuclear dynamics at the balance point.

PACS numbers: 25.70.Pq

I. INTRODUCTION

Heavy-ion collision at intermediate energies is a complex phenomenon that depends crucially on the interplay of the mean field and nucleon-nucleon binary collisions. The dominance of either of these ingredients can shed light on the properties of nuclear matter at the extreme of temperature and density. Among various observables and non-observables in heavy-ion collisions, directed collective flow is considered to be a very important observable due to its extreme sensitivity towards the model ingredients and physics involved [1–3]. The very same observable has also been robust for the understanding of nuclear equation of state - a question that is still open and extensively debated in the literature [4–10]. The directed collective flow has been reported by many authors to be positive at higher incident energies whereas same is deeply negative at low incident energies.

*Electronic address: rkpuri@pu.ac.in

While going from the low to high incident energies, there comes a typical point where no preference is observed for the flow, therefore, it disappears. This particular incident energy where attractive and repulsive interactions balance each other (and flow disappears) is termed as balance energy or E_{bal} [9, 11–18]. At the balance point, scatterings due to the attractive mean field occurring at negative angles are counter balanced by the repulsive action of the binary nucleon-nucleon collisions occur at positive angles [12, 15, 19, 20].

The composite dependence of the E_{bal} on the mean field equation of state (eos) and nucleon-nucleon cross-section (σ_{NN}) can be sorted out by noticing the sensitivity of E_{bal} on the system size as well as on the impact parameter of the reaction. In this connection, very recently, Puri and Sood [19], conducted a very detailed and exhaustive study on the energy of vanishing flow over entire periodic table with masses between 20 and 394. Their study had shed light on various aspects of nuclear dynamics. Unfortunately, this study along with all other studies reported in the literature are limited to central/semi-central collisions only [19]. A very little attention has been paid in the literature for semi-central and/or peripheral collisions, where physics is derived by the low density dynamics [10, 14, 19–23]. Among various attempts involving non-central impact parameters, Magestro et. al. [17] reported the results of disappearance of flow over large impact parameters. Their study, however, was limited to heavier systems only. One should keep in the mind that the dynamics in lighter nuclei is entirely different than that of heavier colliding nuclei. It remains, therefore, a challenging question to see how directed transverse flow behaves at peripheral/non-central collisions. We plan to address this question in this study.

In an another study, Puri et.al. [13] extracted the strength of nucleon-nucleon cross-section for the reaction of $Zn^{64} + Al^{27}$ at different collision geometries. They firmly indicated that for central collisions, a cross-section of 40 mb was good enough, whereas an enhanced value of cross-section was needed for peripheral collisions. It still remains to be seen whether this observation holds good over entire periodic table or not.

Here we plan to understand the mass dependence of disappearance of flow in these low excited geometries. We shall also attempt to parameterize the balance energy for the system size effects. The present study is conducted within the framework of quantum molecular dynamics (QMD) model, which is discussed in section II. In section III, we discuss the results and summary is presented in section IV.

II. THE MODEL

In QMD model [24–26], each nucleon, represented by a Gaussian distribution, propagates with classical equations of motion as:

$$\frac{d\mathbf{r}_i}{dt} = \frac{dH}{d\mathbf{p}_i}, \quad (1)$$

$$\frac{d\mathbf{p}_i}{dt} = -\frac{dH}{d\mathbf{r}_i}, \quad (2)$$

where Hamiltonian H is given by :

$$H = \sum_i \frac{\mathbf{p}_i^2}{2m_i} + V^{tot}, \quad (3)$$

with

$$V^{tot} = V^{loc} + V^{Yuk} + V^{Coul}. \quad (4)$$

Here V^{loc} , V^{Yuk} and V^{Coul} represent, respectively, the local two- and three-body Skyrme, Yukawa and Coulomb interactions. Under the local density approximation, Skyrme part of the nucleon interaction can be written as:

$$V^{loc} = \alpha/2 \sum_i \rho_i + \frac{\beta}{\gamma + 1} \sum_i \rho_i^\gamma. \quad (5)$$

Here ρ_i is the nucleon density. The coefficients α and β give proper ground state properties and γ is used to generate different compressibilities. The different values of compressibility (γ) give possibility to look for the role of different equations of state termed as soft ($\gamma = 200$ MeV) and stiff ($\gamma = 380$ MeV) equations of state. The values of α and β for soft and hard equation of state are -0.356 GeV, 0.303 GeV and -0.124 GeV, 0.0705 GeV [24]. Following many studies [15, 16, 18, 19] listed in the literature, we also use a hard equation of state.

When propagating nucleons come too close to each other, they can collide elastically or inelastically depending upon the available center of mass energy. The collision probability depends on the cross section σ_{NN} . Several different forms of σ_{NN} are available in the literature. In many studies [18, 19], one has taken constant value of σ_{NN} . Generally it is assumed to be between 20 mb and 55 mb. The strength of nucleon-nucleon cross-section will be extracted by simulating various reactions with σ_{NN} between 40 and 55 mb. The above QMD model has been shown to be very useful in many observables/non-observables [25, 26].

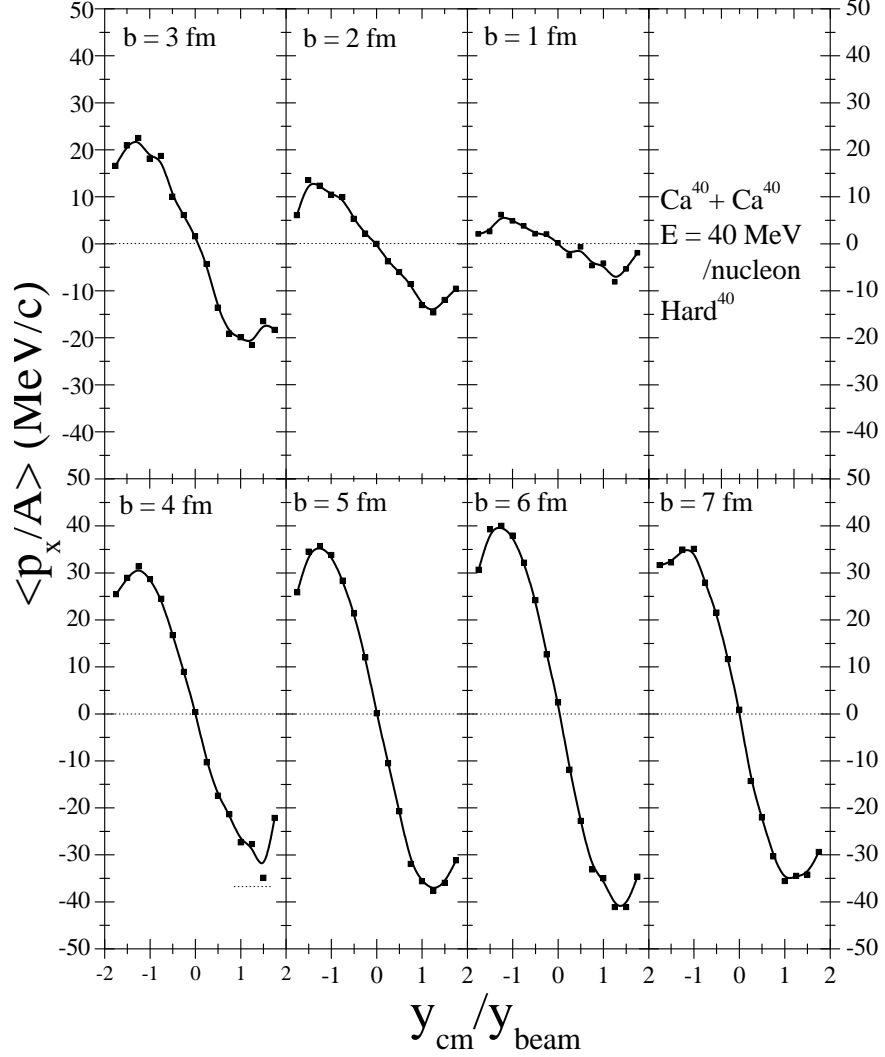


FIG. 1: Average $\langle p_x/A \rangle$ (MeV/c) as a function of scaled rapidity y_{cm}/y_{beam} . We display the results (anticlockwise) at impact parameters $b = 1, 2, 3, 4, 5, 6$ and 7 fm.

III. RESULTS AND DISCUSSION

For the present study, symmetric reactions of $Ne^{20} + Ne^{20}$, $Ca^{40} + Ca^{40}$, $Ni^{58} + Ni^{58}$, $Nb^{93} + Nb^{93}$, $Xe^{131} + Xe^{131}$ and $Au^{197} + Au^{197}$ are taken. The entire colliding geometry is considered with main emphasis on the semi-central as well as on the peripheral collisions. Throughout the present analysis, a hard equation of state along with $\sigma_{NN} = 40 - 55$ mb has been used. In fig.1, we display the changes in the transverse momentum $\langle p_x/A \rangle$ as a function of the rapidity distribution y_{cm}/y_{beam} . Here we vary impact parameter from $b = 1$ to $b = 7$ fm at a step of unity. We see

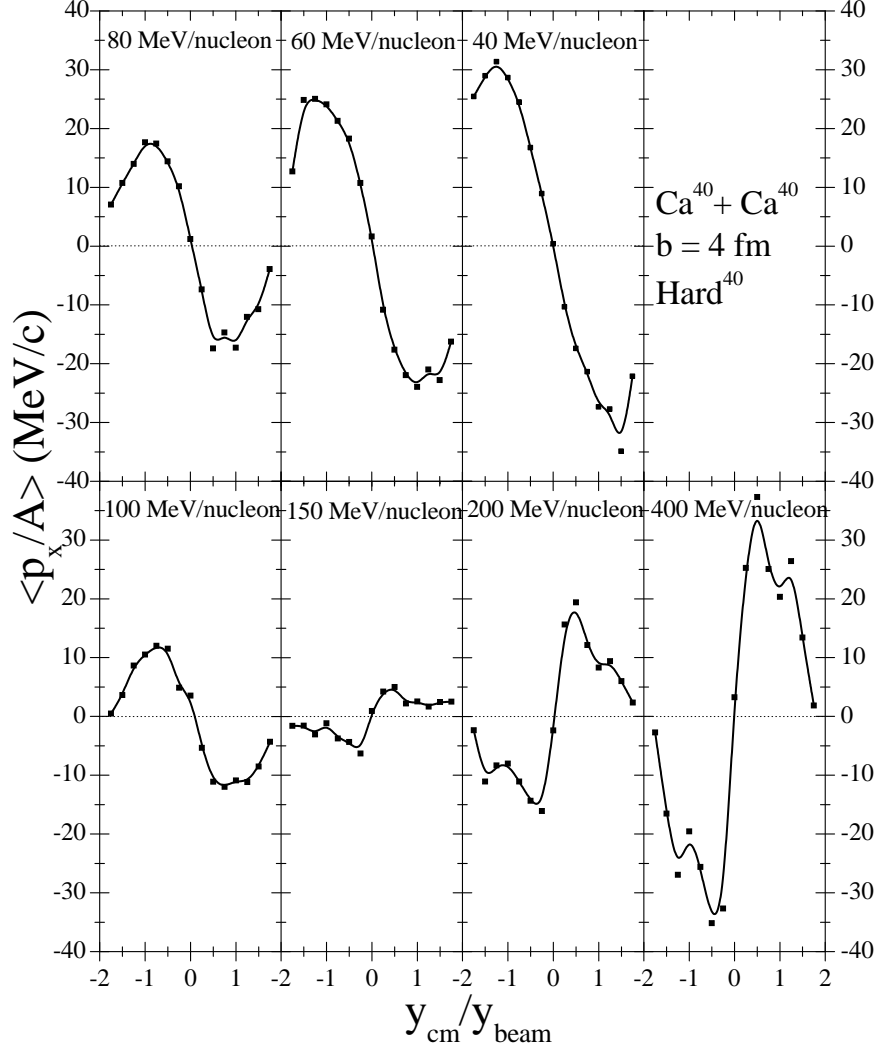


FIG. 2: Same as in fig. 1 but here we display the results (anticlockwise) at energies 40, 60, 80, 100, 150, 200 and 400 MeV/nucleon.

that for $b = 1$ fm, flow is nearly isotropic and slope is zero. The negative slope increases as we move from central to peripheral collisions. This demonstrates that for larger impact parameters, matter is attractive in the presence of reduced number of collisions. It is worth that the slope of the $\langle p_x/A \rangle$ depends crucially on the incident energy. In fig. 2, we display the $\langle p_x/A \rangle$ for the same reaction as fig. 1 but at $b = 4$ fm and for different incident energies. We see that slope is negative at small incident energies whereas it turns less negative with the increase in the incident energies. At particular energy (between 100 and 150 MeV/nucleon), we see a change in the slope

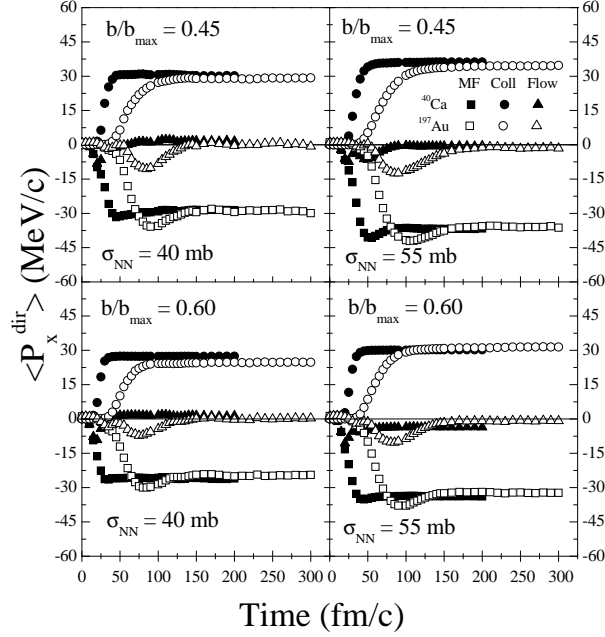


FIG. 3: The time evolution of total directed transverse momentum $\langle P_x^{dir} \rangle$ along with mean field and collision parts at the energy of vanishing flow. Solid symbols represent Ca^{40} whereas open symbols are for Au^{197} .

from negative to positive values. This slope is steeper at higher incident energies.

In Fig.3, the transverse directed momentum, $\langle P_x^{dir} \rangle$ is plotted as a function of reaction time for the collisions of $Ca^{40}+Ca^{40}$ and $Au^{197}+Au^{197}$ using $\sigma_{NN} = 40$ and 55 mb, respectively. The displayed results are at reduced impact parameters b/b_{max} (\hat{b}) = 0.45 and 0.60 . The plots are displayed at the energy of vanishing flow i.e. balance energy. For a better understanding, we divide the total transverse momentum into contribution resulting from the mean field and from the collision parts. From the figure, one observes that the transverse momentum due to mean field (representing squares) is being equated by that due to binary nucleon-nucleon collisions (circles), resulting in net zero flow (triangles) at the end of the reaction. The mean field contribution dominates the reaction during early evolution resulting in negative (attractive) transverse flow. It is worth mentioning that if mean field dominates, the transverse flow will be negative whereas the dominance of nucleon-nucleon collisions will result in to a positive flow. At ultra low incident energies, the phenomena emerging due to mean field alone are dominant [27]. The reaction persists longer for heavier systems (up to 100 fm/c or so for Au^{197}) compared to lighter colliding nuclei (which is about 50 fm/c). This happens due to lower energy of vanishing of flow in heavier systems

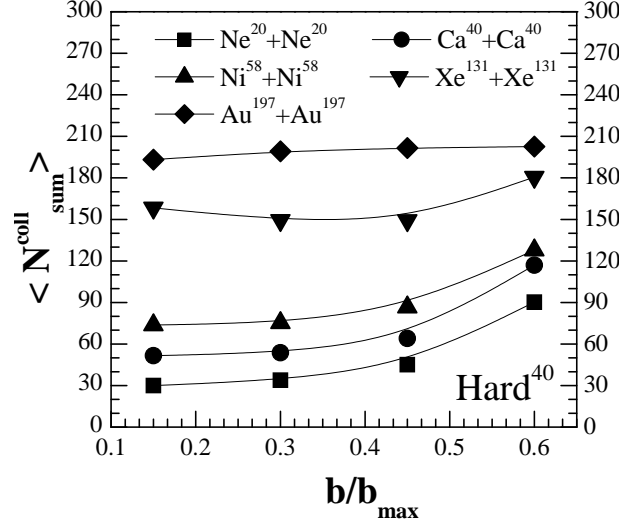


FIG. 4: The total binary collisions ($\langle N_{sum}^{coll} \rangle$) at 200 fm/c as a function of reduced impact parameter (\hat{b}). Lines are drawn to guide the eye. Here the reactions of $\text{Ne}^{20}+\text{Ne}^{20}$, $\text{Ca}^{40}+\text{Ca}^{40}$, $\text{Ni}^{58}+\text{Ni}^{58}$, $\text{Xe}^{131}+\text{Xe}^{131}$ and $\text{Au}^{197}+\text{Au}^{197}$ are taken.

compared to light systems. The different values of the flow due to mean field using different σ_{NN} happens due to different energies of vanishing flow.

We plot in Fig.4, the number of allowed collisions $\langle N_{sum}^{coll} \rangle$, for various systems as a function of reduced impact parameter \hat{b} . This dependence of binary collisions on impact parameter yields several interesting aspects: For the lighter masses, there is a marked enhancement in the binary collisions at peripheral collisions. This happens due to exceedingly high balance energy at these impact parameters in lighter colliding nuclei. For example, the E_{bal} for $\text{Ne}^{20}+\text{Ne}^{20}$ at $\hat{b} = 0.15$ is 76 MeV/nucleon, which goes up to 360 MeV/nucleon for $\hat{b} = 0.60$. On the other hand, binary collisions for heavier colliding nuclei (like $\text{Au}^{197} + \text{Au}^{197}$) are almost independent of the impact parameter. This is due to the fact that the energy of vanishing flow is very small in $\text{Au}^{197}+\text{Au}^{197}$ reaction (between 40 and 78 MeV/nucleon) and at these low incident energies, most of the binary collisions are blocked, and as a result no significant impact parameter dependence is obtained for binary collisions in heavy-ion systems.

In figs.5 and 6, we plot the energy of vanishing flow as a function of total system mass A (mass of projectile + mass of target) for entire mass range between 40 and 394 units. Remarkably, our present calculations with σ_{NN} between 40 and 55 mb explain experimental data for $\hat{b} = 0.45$ nicely, whereas some deviation appears in the case of $\hat{b} = 0.60$. The data shown in the figure are for the

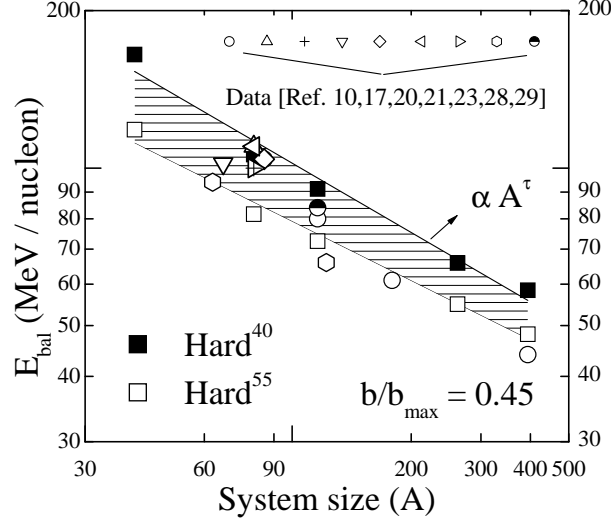


FIG. 5: The balance energy as a function of system mass at $\hat{b} = 0.45$. The data points are taken from references mentioned in text. Shaded region represents the energy of vanishing flow obtained with $\sigma_{NN} = 40$ and 55 mb

reactions of $Ar^{40} + Sc^{45}$, $Ca^{40} + Ca^{40}$, $Ni^{58} + Ni^{58}$, $Fe^{58} + Fe^{58}$, $Kr^{86} + Nb^{93}$, $Ar^{36} + Al^{27}$, $Zn^{64} + Ni^{58}$, $Zn^{64} + Ti^{48}$ and $Au^{197} + Au^{197}$ [10, 17, 20, 21, 23, 28, 29]. The scarcity of data at larger impact parameters restricts the similar detailed analysis. We notice that different cross-sections have larger influence for light colliding nuclei that reduces significantly for heavier systems. The cause suggests the fact that the balance energy for heavier system is much smaller compared to lighter nuclei. As a result, cross-section plays an insignificant role in heavier systems. This mass dependence can be parameterized by a power law of the form $\propto A^\tau$. As we see, the τ for $\hat{b} = 0.45$ is -0.44 and -0.37 for our calculations with $\sigma_{NN} = 40$ and 55 mb respectively, whereas it is -0.66 and -0.57 for $\sigma_{NN} = 40$ and 55 mb at $\hat{b} = 0.60$. The deviation of our calculated energy of vanishing flow from experimental data suggests that the dynamics of low energy domain needs further investigation. We also notice that around $A = 100$ units, no clear mass dependence appears. This could also be due to the fact that impact parameter in these measurements is not fixed. It varies with reaction. The impact parameter variation can also have effect on the energy of vanishing flow.

Fig.7 shows our calculated balance energy versus system mass at reduced impact parameters of 0.15 , 0.30 , 0.45 and 0.60 . All calculated points in the energy scale are fitted with a power law $\propto A^\tau$. One notice that the slope of plots increases with impact parameter. The values of power

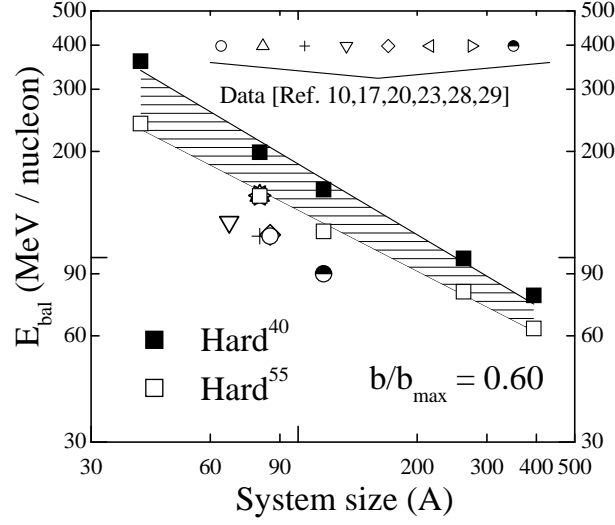


FIG. 6: Same as fig.5, but at $\hat{b} = 0.60$.

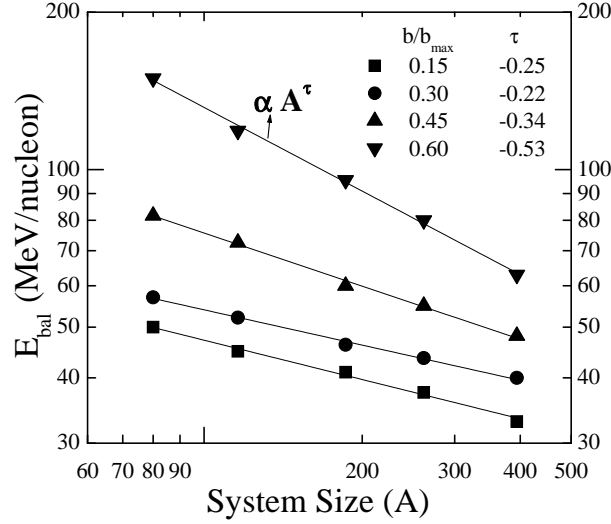


FIG. 7: The balance energy E_{bal} against system mass at different reduced impact parameters. The displayed results are using QMD model with hard EOS at 55 mb cross-section.

factor τ are -0.25, -0.22, -0.34 and -0.53 respectively, for $\hat{b} = 0.15, 0.30, 0.45$ and 0.60 (Note that in this figure and fitting, $Ne^{20} + Ne^{20}$ reaction has been excluded, therefore slope deviates slightly compared to fig.6). We see that the value of τ depends strongly on the colliding geometry. For instance, for central collisions, E_{bal} is 50-57 MeV/nucleon for $Ca^{40} + Ca^{40}$ reaction, whereas it

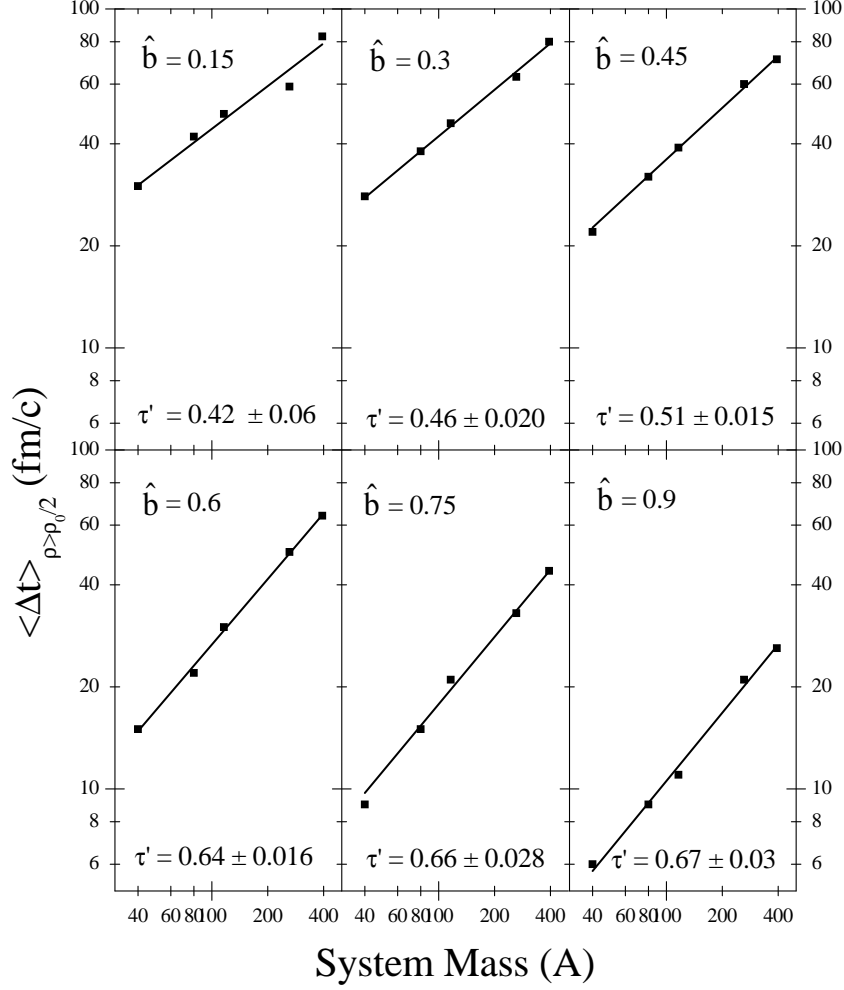


FIG. 8: The time zone for which density remains higher than half of the normal matter versus system size for different impact parameters.

increases to 149.5 MeV/nucleon for $\hat{b} = 0.60$.

For central collisions, we observe that the power factor is close to $(-1/3)$. This is a well known trend reported by number of authors earlier [11, 18, 19] and has been very well justified in the literature in terms of interplay between the mean field and binary collisions. The increase in the slope of E_{bal} with impact parameter can be due to failure of static equation of state to reproduce transverse motion of particles. The effect is more severe for lighter nuclei. This is partially due to the fact that with weaker binary nucleon-nucleon collisions, Coulomb's repulsion plays a decisive

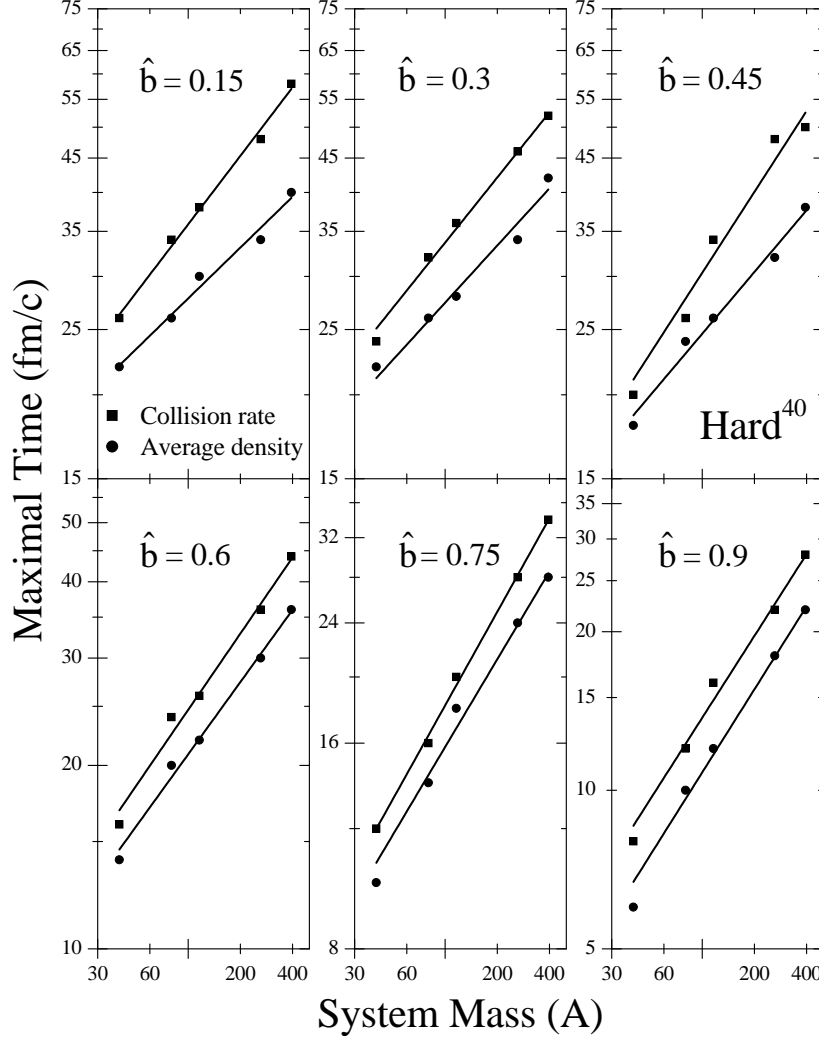


FIG. 9: Maximal time for collision rate and average density as function of system size.

role. This role is very strong in heavier nuclei and at peripheral collisions, therefore making slope steeper. It still remains to be seen how momentum dependent interactions can alter these findings.

To further understand this similarity in the balance energy obtained at different impact parameters, we display in fig.8, the evolution time for which density remains higher than half of the matter density i.e. the time for which $\rho > 0.5\rho_0$. This gives an important information about the interaction time at different impact parameters. We display the results at $\hat{b} = 0.15$, $\hat{b} = 0.3$, $\hat{b} = 0.45$, $\hat{b} = 0.6$, $\hat{b} = 0.75$ and $\hat{b} = 0.9$. Interestingly, we see that in all cases, time zone for different masses can be explained with the help of a power law $\propto c'A^{\tau'}$. The factor τ' increases systemati-

cally from central to peripheral reactions. It is 0.42 for central whereas it increases to 0.67 for $\hat{b} = 0.9$. A careful look reveals that the effect is less for heavier nuclei (for Au+Au it is 80 fm/c for $\hat{b} = 0.15$ whereas, it is 20 at $\hat{b} = 0.9$). On the other hand, it has drastic effect for lighter one where it slashes to 10% of central values. This is the cause why balance energy changes drastically for lighter nuclei compared to heavier ones and we have different slopes compared to peripheral ones.

In fig.9, we display the maximal time of average density and collision rate for the same systems as shown in fig.8. Here we also see again a similar trend as seen in fig.8. There is a monotonous increase in the slope from central to peripheral collisions.

IV. SUMMARY

In the present work, we analyzed the disappearance of flow (or alternately the balance energy) for semi-central and peripheral collisions using quantum molecular dynamics model. The present study was undertaken by using a hard equation of state along with constant cross-sections between 40 and 55 mb. We see a mass dependence $\propto A^{-1/3}$ for central collisions, whereas this dependence becomes steeper with impact parameter. This deviation from -1/3 trend suggests exceeding role of Coulomb's repulsion in low density and excited situations. Nuclear dynamics at the balance point indicates drastic changes in lighter system compared to heavy one in agreement with balance energy.

This work is supported by Department of Science and Technology, Government of India.

-
- [1] N. Herrmann, J. P. Wessels and T. Wienold, *Annu. Rev. Nucl. Part. Sci.* **49** (1999) 581.
 - [2] H. A. Gustafsson *et al.*, *Phys. Rev. Lett.* **52** (1984) 1590.
 - [3] R. E. Renforst *et al.*, *Phys. Rev. Lett.* **53** (1984) 763.
 - [4] C. Hartnack, R. K. Puri, J. Aichelin, J. Konopka, S. A. Bass, U. Stöcker and W. Greiner, *Eur. Phys. J. A1* (1998)151.
 - [5] A. Andronic *et al.*, *Phys. Rev. C* **67** (2003) 034907.
 - [6] H. Stöcker and W. Greiner, *Phys. Rep.* **137** (1986)277.
 - [7] D. H. Rischke, *Nucl. Phys. A***610** (1990) 88c.
 - [8] Q. Pan and P.Danielewicz, *Phys. Rev. Lett.* **70** (1993) 2062.
 - [9] H. Zhou, Z. Li, Y. Zhuo and G. Mao, *Nucl. Phys. A* **580** (1994) 627.
 - [10] J. P. Sullivan *et al.*, *Phys. Lett. B* **249** (1990) 8.
 - [11] G. D. Westfall *et al.*, *Phys. Rev. Lett.* **71** (1993) 1986.

- [12] D. Krofcheck *et al.*, *Phys. Rev. C* **43** (1991) 350.
- [13] S. Kumar, M. K. Sharma, R. K. Puri, K. P. Singh and I. M. Govil, *Phys. Rev. C* **58** (1998) 3494.
- [14] C. Ogilvie *et al.*, *Phys. Rev. C* **42** (1990) R10.
- [15] D. Krofcheck *et al.*, *Phys. Rev. C* **46** (1992) 1416.
- [16] Z. Y. He *et al.*, *Nucl. Phys. A* **598** (1996) 248(R).
- [17] D. J. Majestro, W. Bauer and G. D. Westfall, *Phys. Rev. C* **62** (2000) 041603.
- [18] Aman D. Sood and R. K. Puri, *Phys. Lett. B* **594** (2004) 260 and references therein.
- [19] Aman D. Sood and R. K. Puri, *Phys. Rev. C* **69** (2004) 054612 and references therein.
- [20] Sven Soff *et al.*, *Phys. Rev. C* **51** (1995) 3320.
- [21] A. Buta *et al.*, *Nucl. Phys. A* **584** (1995) 397.
- [22] J. Molitoris and H. Stocker, *Phys. Lett.* **162B** (1985) 47.
- [23] R. Pak *et al.*, *Phys. Rev. C* **53** (1996) 1469.
- [24] J. Aichelin, *Phys. Rep.* **202** (1991) 233.
- [25] Y. K. Vermani and R. K. Puri, *J. Phys. G* **36** (2009) 105103; Y. K. Vermani *et al.*, *J. Phys. G* **37** (2010) 015105; Y. K. Vermani, S. Goyal, and R. K. Puri *Phys. Rev. C* **79** (2009) 064613; Y. K. Vermani and R. K. Puri, *Eur. Phys. Lett.* **85** (2009) 62001; A. D. Sood and R. K. Puri, *Phys. Rev. C* **79** (2009) 064618; S. Kumar, S. Kumar, and R. K. Puri, *Phys. Rev. C* **78** (2008) 064602.
- [26] D. T. Khoa *et al.*, *Nucl. Phys. A* **619** (1992) 102; S. W. Huang *et al.*, *Phys. Lett. B* **298** (1993) 41; C. Batko, A. Faessler, S. W. Huang, E. Lehmann, and R. K. Puri, *J. Phys. G* **20** (1994) 461; E. Lehmann, R. K. Puri, A. Faessler, G. Batko, and S. W. Huang, *Phys. Rev. C* **51** (1995) 2113; E. Lehmann *et al.*, *Prog. Part. Nucl. Phys.* **30** (1993) 219; S. W. Huang *et al.*, *Prog. Part. Nucl. Phys.* **30** (1993) 105; R. K. Puri, C. Hartnack, and J. Aichelin, *Phys. Rev. C* **54** (1996) R28; R. K. Puri and J. Aichelin, *J. Comput. Phys.* **162** (2000) 245; R. K. Puri, *et al.*, *Nucl. Phys. A* **575** (1994) 733.
- [27] S. S. Malik *et al.*, *Pramana J. Phys.* **32** (1989) 419; R. K. Puri *et al.*, *Euro. phys. Lett.* **9** (1989) 767; R. K. Gupta, S. Singh, R. K. Puri and W. Scheid, *Phys. Rev. C* **47** (1993) 561; R. K. Puri, P. Chattopadhyay, R. K. Gupta, *Phys. Rev. C* **43** (1991) 315; R. K. Puri *et al.*, *Eur. Phys. J. A* **23** (2005) 429; R. Arora *et al.*, *Eur. Phys. J. A* **8** (2000) 103.
- [28] R. Pak *et al.*, *Phys. Rev. C* **54** (1996) 2457.
- [29] G. D. Westfall, *Nucl. Phys. A* **681** (2001) 343c.